Discrimination of wide-field images as a test of a peripheral-vision model

Eli Peli

Schepens Eye Research Institute, Harvard Medical School, Boston, Massachusetts 02114

George A. Geri

L-3 Communications Corporation, 6030 South Kent, Mesa, Arizona 85212

Received March 13, 2000; accepted August 8, 2000; revised manuscript received August 17, 2000

In order to test a model of peripheral vision, various contrast sensitivity functions (CSF's) and fundamental eccentricity constants (FEC's) [see J. Opt. Soc. Am. A **8**, 1762 (1991)] were applied to real-world, wide-field (6.4°–32° eccentricity) images. The FEC is used to model the change in contrast sensitivity as a function of retinal eccentricity. The processed test images were tested perceptually by determining the threshold FEC for which the observers could discriminate the test images from the original image. It was expected that higher CSF sensitivity would be associated with higher FEC's; and in fact, for images processed with low-pass (variable-window stimuli) CSF's, the threshold FEC's were larger for the higher-sensitivity (pattern-detection) CSF than for the lower-sensitivity (orientation detection) CSF. When two higher-sensitivity CSF's were compared, the bandpass (constant-window stimuli) CSF resulted in essentially the same FEC threshold as did the low-pass (variable-window stimuli) CSF. The fact that the FEC compensated for complex differences in the form of the CSF suggested that the discrimination task was mediated by a limited range of spatial frequencies over which the two CSF's were similar. Image contrast was then varied in order to extend the range of spatial frequencies tested. The FEC's estimated with the lower-contrast test images were unchanged for test images obtained with the high-sensitivity, bandpass CSF but increased for test images obtained with the high-sensitivity, low-pass CSF. These results suggest that peripheral contrast sensitivity as used in the present discrimination task is based on a high-sensitivity, bandpass CSF. The peripheral-vision model validated by the present analysis has practical applications in the evaluation of wide-field simulator images as well as area-of-interest or other foveating systems.

OCIS codes: 330.4060, 330.1800, 330.1880, 330.5000, 330.6100, 330.6110.

1. INTRODUCTION

Computational vision models have been used to predict the discrimination and the appearance of images and scenes in a variety of experimental contexts.[1–7] One such multiscale model of spatial vision was used to calculate local band-limited contrast in complex images.[8] This contrast measure along with the observers' contrast sensitivity functions (CSF's) were used to simulate the appearance of images to observers with both normal[8] and low[7] vision. Others have used variations of the concept of local band-limited contrast for similar purposes.[6,9,10] The local band-limited contrast model has also been used along with the CSF measured at various retinal eccentricities to simulate the appearance of images presented in the visual periphery.[11]

Peli[12] simulated the appearance of complex images using a local band-limited contrast model and demonstrated the validity of the model for central ($\leq 2°$ eccentricity) vision. In that study, observers were asked to discriminate an original image from a processed image that represented how the original would appear when viewed from various distances. The distance at which discrimination performance was at threshold was found to match the simulated observation distance. Peli[12] also determined that CSF data obtained with 1-octave Gabor patches and a detection task were the most appropriate for use in the context of the tested vision model. In a recent study[13] these results were expanded by applying the same vision model to versions of the same images that differed in contrast. In the present study we used a similar model to test images that extended farther into the visual periphery, and we used a similar testing method to evaluate the discrimination of test images obtained with different CSF's. We also varied image contrast in order to test each CSF over a wider range of spatial frequencies.

Spatial inhomogeneity, in the form of nonuniform processing and nonuniform organization as a function of eccentricity, is a salient feature of the human visual system and has been documented at various levels in the visual pathway.[14] Peli *et al.* showed that the changes in contrast sensitivity across the retina might play an important role in maintaining size (distance) invariance.[11] The property of the visual system that underlies the (suboptimal) invariance of perceived image contrast with changes in image size—associated, for instance, with changes in image distance—should be included in visual models. In particular, spatial nonuniformity cannot be ignored when a model is applied to wide-field images.

In the present study we have used the pyramidal, local-band-limited contrast model described previously,[8,11] as well as known variations in contrast sensitivity across the visual field,[11,15,16] to test a generalization of our model to wide-field (6.4°–32°) images. The model, which incorporates changes in contrast sensitivity as a function of ec-

centricity, is based on the foveal CSF and a single additional parameter, the fundamental eccentricity constant (FEC). The FEC is used to model the change in contrast sensitivity as a function of retinal eccentricity.[11] Specifically, the FEC is the slope of the function relating log contrast threshold to retinal eccentricity as measured with a 1 cycle per degree (c/deg) stimulus. For other spatial frequencies, the slope of the function is the product of the FEC and the spatial frequency. If this approach can be validated, it would suggest that peripheral discrimination of wide-field images could be modeled by using a very simple measure of the change in contrast sensitivity with retinal eccentricity. The purposes of the present study were to determine whether a single eccentricity-dependent parameter (i.e., the FEC) is sufficient to model the spatial nonuniformity of the visual system and to determine which of several CSF's is most appropriate for modeling the discrimination of complex, wide-field images.

2. METHODS

A. Observers

Six observers were tested, although not all under all experimental conditions. The observers ranged in age from 18 to 48 years and had uncorrected 20/20 vision as determined by a Snellen chart. The observers were paid for their participation.

B. Stimulus and Apparatus

1. Test-Image Processing: General

Four test images were obtained from the left and right halves of two digitized aerial photographs, one of an airport and the other of planes on the ground (see Fig. 1). The details of the method used to process the test images are given in Ref. 8, and the modifications used to process the test images as a function of eccentricity are given in Ref. 11. Briefly, a series of bandpass images was generated by processing an original image with the use of a series of nonoriented bandpass filters, each with a 1-octave full bandwidth (half-amplitude) and separated by 1 octave. A series of low-pass images was then generated by summing all of the bandpass images below each of the bandpass levels. A series of local band-limited contrast images was then obtained by dividing the value of each point in each bandpass image by the value of the corresponding point in the corresponding low-pass image.[8] Next, a fixation locus was assigned at the center of the local band-limited contrast image, and the distance from the fixation locus was determined for each point in the image. On the basis of that distance (in degrees) and of the spatial frequency associated with each bandpass image, a thresholded bandpass image was obtained by testing each point in each local band-limited contrast image against an appropriate threshold [see Eq. (1)] at that point, to determine whether the point was visible. If the point was found to be above threshold, the corresponding point in the corresponding bandpass image was placed in the thresholded bandpass image; if not, the corresponding point was set to zero. Finally, the test images were generated by summing the thresholded bandpass images for all bandpass levels.

In the present study, the criterion threshold referred to above was based on the following peripheral-vision model:

$$T(\theta, f) = T(0, f)\ \exp(\mathrm{FEC}\theta f), \tag{1}$$

where θ is eccentricity, f is the radial spatial frequency in cycles per degree, $T(0, f)$ is the foveal threshold [i.e., the inverse of the functions shown in Fig. 2(a)], and FEC is the fundamental eccentricity constant. Test images were generated by using various criterion thresholds each obtained from Eq. (1) with the use of one of three foveal CSF data sets [see Fig. 2(a)] and one of seven FEC levels (see below). The first CSF was based on the orientation discrimination of horizontal and vertical 1-octave Gabor patches (i.e., a sinusoid within a Gaussian aperture whose width varied with spatial frequency). This CSF has a relatively low peak sensitivity and is low-pass in

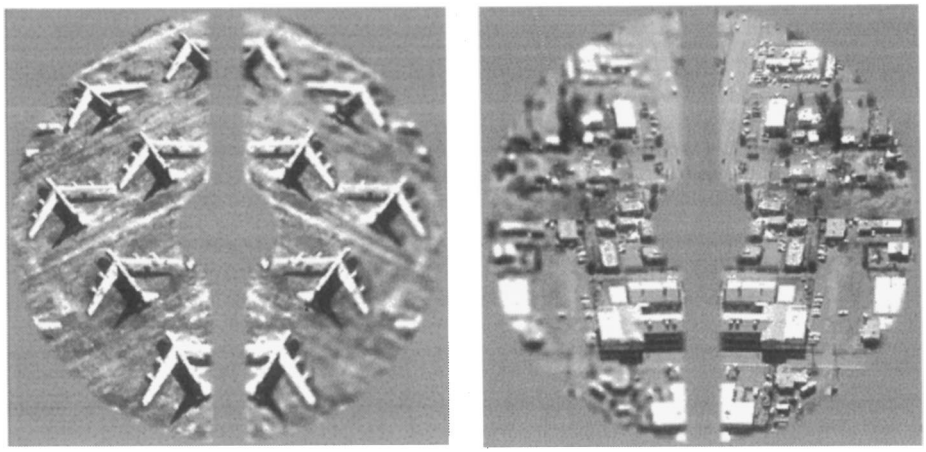

(a) (b)

Fig. 1. Typical test stimuli used in the image discrimination study. The images shown here were obtained by applying (a) an FEC level of 0.15 to the right side of the mirror-image pair derived from the right side of the planes image and (b) an FEC level of 0.20 to the left side of the mirror-image pair derived from the left half of the airport image. Only the two highest FEC levels are depicted here since lower levels are difficult to see in printed images.

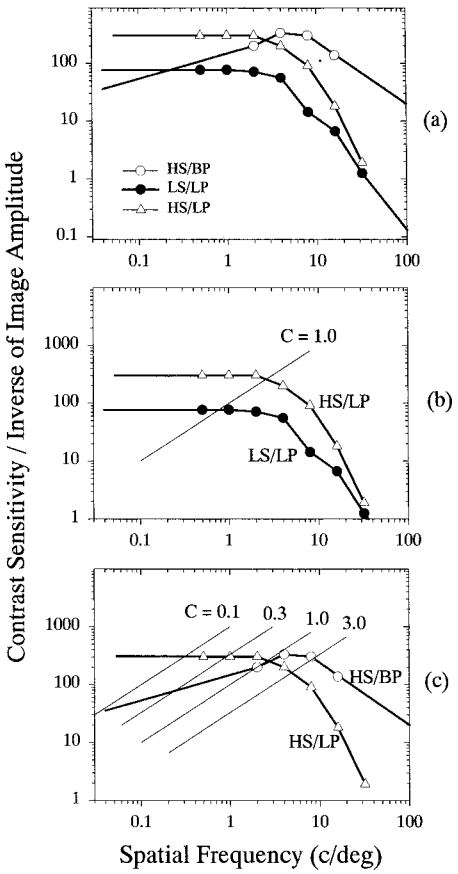

Fig. 2. (a) The three CSF data sets used to produce the present test images. The low sensitivity/lowpass (LS/LP) set was obtained with Gabor stimuli in an orientation discrimination task. The high sensitivity/low-pass (HS/LP) set was obtained with the same stimuli in a contrast detection task. The high sensitivity/bandpass (HS/BP) set was obtained with fixed-aperture grating stimuli in a detection task. The HS/BP CSF was extrapolated to lower frequencies by using a straight line of slope 0.5, and to higher frequencies by extending the line segment connecting the two highest-frequency points. The spatial frequencies corresponding to the high-frequency extrapolation were not present in the test images used here. (b) The HS/LP and LS/LP CSF's and a function that approximates a $1/f$ image amplitude spectrum whose contrast, C, has been designated as 1.0 (see Section 4). (c) The HS/BP and HS/LP CSF's and a series of functions that approximate relative $1/f$ amplitude spectra of images whose contrasts vary by the factors shown and that were used as test stimuli in the present study (see Section 4).

character, and so it has been designated low sensitivity/low pass (LS/LP). This CSF was measured by Peli *et al.*[11] foveally and at various eccentricities and was shown to fit the peripheral model with a single FEC (0.048 and 0.058 for the two subjects). The second CSF was obtained by using a pattern- (contrast-) detection task and the same 1-octave Gabor patches mentioned above. It has a relatively high peak sensitivity, is also low pass, and has been designated high sensitivity/low pass (HS/LP). The same stimuli and task were used to measure the CSF at various retinal eccentricities by Pointer and Hess,[17] and the resulting data were well fitted by a model with an FEC of 0.03. Peli[12] also found this same CSF to best represent image discrimination performance foveally. Finally, the third CSF was based on the pattern detection of sinusoid gratings within a 2° square aperture.[18] It has a relatively high peak sensitivity, is bandpass in character, and has been designated high sensitivity/bandpass (HS/BP). This CSF was measured foveally and at various eccentricities by Cannon,[18] and the data were also found by Peli *et al.*[11] to fit the single FEC (0.035) peripheral model well.

Whenever values outside the CSF measurement range were needed to produce the test images, they were extrapolated as shown in Fig. 2(a). The relationship between the characteristics of the various CSF's and the stimuli and psychophysical techniques used to obtain them are summarized in Table 1. The FEC levels tested were 0.02, 0.035, 0.055, 0.075, 0.10, 0.15, and 0.20. These levels were selected to span the values of approximately 0.030–0.057 that had previously been found[11] to fit various peripheral CSF data sets from the literature. The range was extended on the high side on the basis of the results of pilot experiments.

2. Test-Image Processing: Contrast Experiments

In a second experiment, the contrast of the original test images was varied so that the image amplitude spectra could be made to intersect the CSF's at various spatial frequencies. The contrast of the test images was varied by subtracting the mean luminance level from the image, multiplying each pixel by the corresponding contrast factor (0.1, 0.3, 0.5, or 3.0), and then adding back the mean luminance. (The 3.0 contrast image was saturated wherever the dark or the bright values exceeded the dynamic range of the display.) As a practical matter, this procedure actually changes the amplitude of the images by a fixed factor. This operation, in which the image dc value is subtracted and the remaining values are scaled up or down, is frequently referred to as a contrast change. As was pointed out by Peli,[8] however, the magnitude of the changes in amplitude are equivalent to the changes in contrast only when the local luminance is equal to the mean luminance. Although the procedure used here does not result in a uniform contrast change at all frequencies and locations, it was sufficient to modify the test images for the purposes of the present study. We use the term contrast change here for consistency with previous work.

Table 1. Sensitivity and Passband Characteristics of the CSF's Used to Process the Test Stimuli of the Present Study, and the Psychophysical Technique and Spatial Window of the Stimuli Used to Obtain Those CSF's

CSF Characteristics	Technique/Stimulus Window Used to Obtain CSF
High Sensitivity/Bandpass (HS/BP)	Pattern Detection/ Constant Window (Square-Wave)[a]
High Sensitivity/Low Pass (HS/LP)	Pattern Detection/ Variable Window (Gaussian)[b]
Low Sensitivity/Low Pass (LS/LP)	Orientation Detection/ Variable Window (Gaussian)[c]

[a] Ref. 18.
[b] Ref. 12.
[c] Refs. 11 and 23.

3. Test Stimuli

Test stimuli (see Fig. 1) were obtained by pairing one half of an unprocessed version of each original test half image with a mirror image of itself, processed as described above. The full test stimuli were $1024 \times 1024 \times 8$ bits and subtended 64° at a viewing distance of 1.2 m. The central 12.8° of each stimulus, a 3.7° vertical strip between the two half-images, and the area outside of a 32°-radius circle were replaced with a homogeneous field whose luminance was equal to the mean luminance of the stimulus images. Although these stimuli contained no information above 8 c/deg, the size of the central mask ensured that the observer's peripheral retina had to be used, thus rendering the higher frequencies undetectable even at high contrasts.

Because the test stimuli were obtained from test images that had been cut out to the above-stated dimensions after they were processed, it was necessary to smooth the edges to reduce spurious high spatial frequencies. The edges (±25 pixels) were smoothed by first subtracting the mean luminance of the entire image from each pixel value, multiplying the result by a cosine function (centered on the edge), and then adding back the mean luminance.

The mean luminance of the test stimuli was ~4 cd/m^2. The gray scale of each stimulus was linearized (i.e., gamma corrected) by use of a look-up table.

4. Apparatus

Stimuli were rear projected onto a large screen (Lumiglas 130, Stewart Film Screen Corp.) by using the green channel of a Barco Graphics 808s CRT projector. Owing to the gain and other directional properties of the rear-projection screen, there was a significant decrease in luminance from the center to each edge of the stimuli. To compensate for this, the gray-scale value of each interior pixel was reduced by a factor that produced a match to the luminance of a pixel of the same digital value at the outer edge of the stimuli. Stimulus presentation and data collection were controlled by an SGI Crimson workstation. Observers were positioned in a chin- and headrest and responded by depressing either the left or the right button on a mouse.

C. Testing Procedure

Before the first formal session, observers were shown several stimulus images so that they could compare the processed and the unprocessed halves of each. All sessions began with 8–10 min of adaptation to a 64° × 64°, homogeneous, mean-luminance field (with a dark, central fixation point) just large enough to contain the circular test image. The observer then initiated the session by depressing the center mouse button. The first stimulus image appeared after ~4 s, and the observer was asked to respond, by depressing either the right or the left mouse button, as to whether the right or the left half of the image appeared more processed (i.e., blurred). Subsequent stimuli were presented 3 s after each response. The stimulus duration was 300 ms. The mean-luminance adapting field and the fixation point were present whenever a stimulus image was not. Response feedback was provided by a tone that was presented following each incorrect response. The first two to five sessions were considered practice, with the exact number determined by when detection performance had appeared to reach an asymptote. The observer's eye position was not monitored, but the data from all observers were similar and were consistent across sessions. In addition, there was no advantage in the context of the present task of not maintaining fixation at the center of the image.

A total of 560 trials were run in each 1-hr session. The 560 trials corresponded to 10 presentations of each of 56 stimulus images (i.e., 4 original images × 2 sides for the standard × 7 FEC levels) in random order. Thus for each session forty responses were used to estimate a percent correct for each image type (airport or planes) at each of the seven FEC levels. Only one image set (LS/LP, HS/BP, or HS/LP) was tested in each session.

D. Data Analysis

Each data point presented here is the mean of between four and eight percent-correct estimates, each obtained from a subset of forty responses within an individual session. Two parameters, F and s, were estimated by fitting the percent-correct data, plotted as a function of FEC level, with a Weibull distribution[19] of the form

$$P = 100 - 50 \exp\left[-\left(\frac{\mathrm{FEC}}{F}\right)^{s}\right], \qquad (2)$$

where P is the percentage of correct responses, FEC is the fundamental eccentricity constant, the factor $(100 - 50)$ is the percent correct at the lower asymptote of the fitted function, F is the FEC value corresponding to a percent correct of 81.6, and s determines the steepness of the fitted function.[20]

3. RESULTS

For comparison with the present data, we have reproduced in Fig. 3 preliminary results that have been previously reported.[21,22] These data show the percentage of correct discriminations as a function of the FEC level applied to one side of the test image. The upper graph of Fig. 3 shows that the test stimuli based on the HS/BP and HS/LP CSF's resulted in different discrimination functions. Similarly, as shown in the lower graph of Fig. 3, different discrimination functions were found for the planes and the city images. The planes image used in the earlier study was identical to that used in the present study [see Fig. 1(a)], whereas the city image was originally chosen to provide more homogeneously distributed detail, and in that respect it differed somewhat from the airport image of the present study. The two data sets in each graph of Fig. 3 differ both in their threshold FEC values (indicated by the dashed vertical lines) and in the lower asymptotes of the functions fitted to the data.

Shown in Fig. 4 is a comparison of the discrimination functions obtained in the present study for the two image types. The individual data points in the figure are means of eight percent-correct estimates: four obtained with the HS/BP CSF and four obtained with the LS/LP CSF. The images of the present study differed from those used by Peli and Geri,[21] and Peli[22] in that the high-

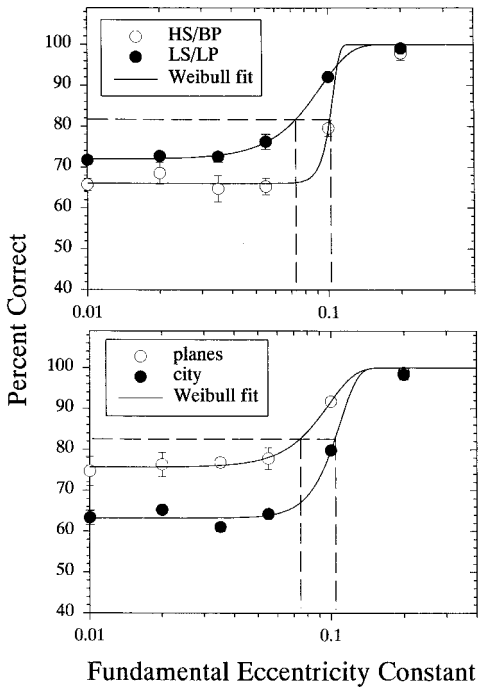

Fig. 3. Preliminary results reported in Peli and Geri[21] and Peli.[22] The smooth curves in the graph represent the best-fitting, three-parameter Weibull function [i.e., not Eq. (2), since the lower asymptote was estimated rather than fixed at 50%]. The data fall on the active part of the psychometric function, and the FEC found is close to the prediction. However, the percent correct is high even for the lowest FEC levels (top graph), and the data display a clear image dependence (bottom graph). These two aspects of the data are not in agreement with the predictions of the vision model tested here.

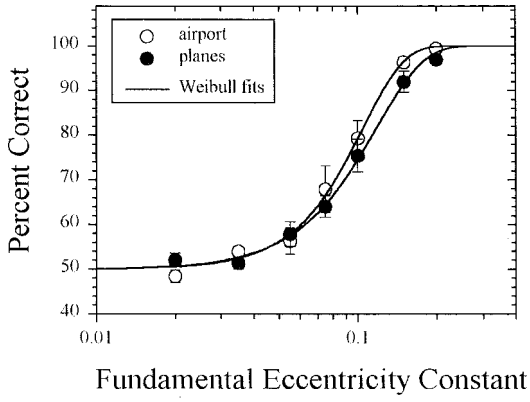

Fig. 4. Discrimination data obtained with images from which the HFR has been removed. The smooth curves correspond to the best-fit, two-parameter Weibull function. The data are means obtained over four observers under the high-sensitivity/bandpass (HS/BP) and low-sensitivity/low-pass (LS/LP) conditions. The error bars are ±1 standard error of the mean (s.e.m.) intervals.

frequency residual (see Section 4) was removed and in that the edges of the images were smoothed as described earlier. The discrimination functions for the two images are now much more similar than the comparable functions shown in the lower graph of Fig. 3 (see Section 4), although there remains a small difference at the higher FEC levels. This difference was evident, however, for only one of the four observers whose data were averaged to produce the functions shown in Fig. 4.

Shown in Fig. 5(a) are the functions relating percent correct to FEC level for test images produced with either the HS/BP (circles) or the HS/LP (triangles) CSF functions. These data represent averages for four observers. The FEC level corresponding to 81.6 percent correct was 0.128 for the HS/BP data and 0.140 for the HS/LP data. Analogous data comparing the results for the HS/LP and the LS/LP CSF functions are shown in Fig. 5(b). The average threshold FEC level for the LS/LP data was estimated to be 0.091. The HS/LP data were obtained for three of the four observers from which the HS/BP and the LS/LP data were obtained. In all cases, the FEC found in our experiments was higher than the 0.030–0.057 value we computed from a number of data sets published in the literature, where grating targets on a uniform background were used.[11]

A further test of the present model was performed by shifting the test-image amplitude spectrum such that it intersected the CSF's at points where their sensitivities differed.[13] The spectrum was shifted by the contrast change procedure described in Section 2. The discrimination data are shown in Fig. 6 for test images whose amplitude spectra were scaled by factors of 0.1, 0.3, 1.0, and 3.0. The results for the original image [Contrast (C) = 1.0) show little difference between the HS/LP and the HS/BP conditions. The differences noted for other contrast levels are addressed in Subsection 4.B.2.

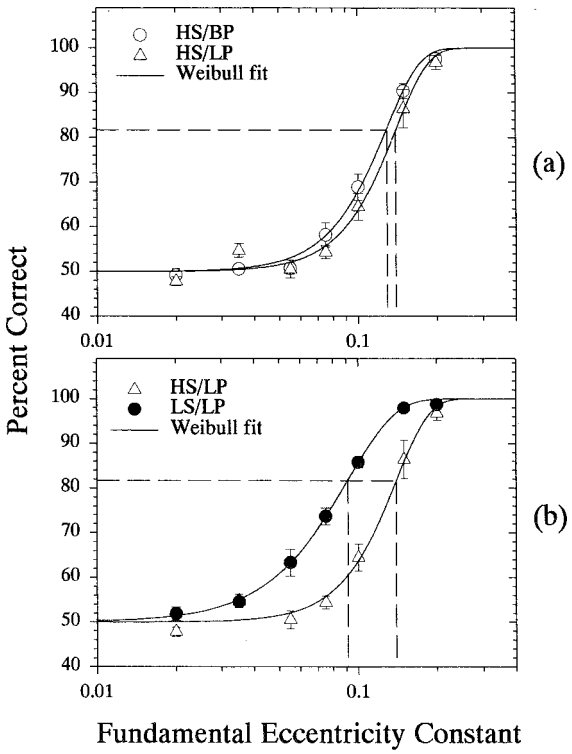

Fig. 5. Comparison of data from test images obtained with the high-sensitivity/bandpass (HS/BP) and the high-sensitivity/low-pass (HS/LP) (top graph) or the high-sensitivity/low-pass (HS/LP) and low-sensitivity/low-pass (LS/LP) (bottom graph) CSF functions. The smooth curves correspond to the best-fit, two-parameter Weibull function. The data are means obtained over four observers, and the error bars are ±1 s.e.m. intervals.

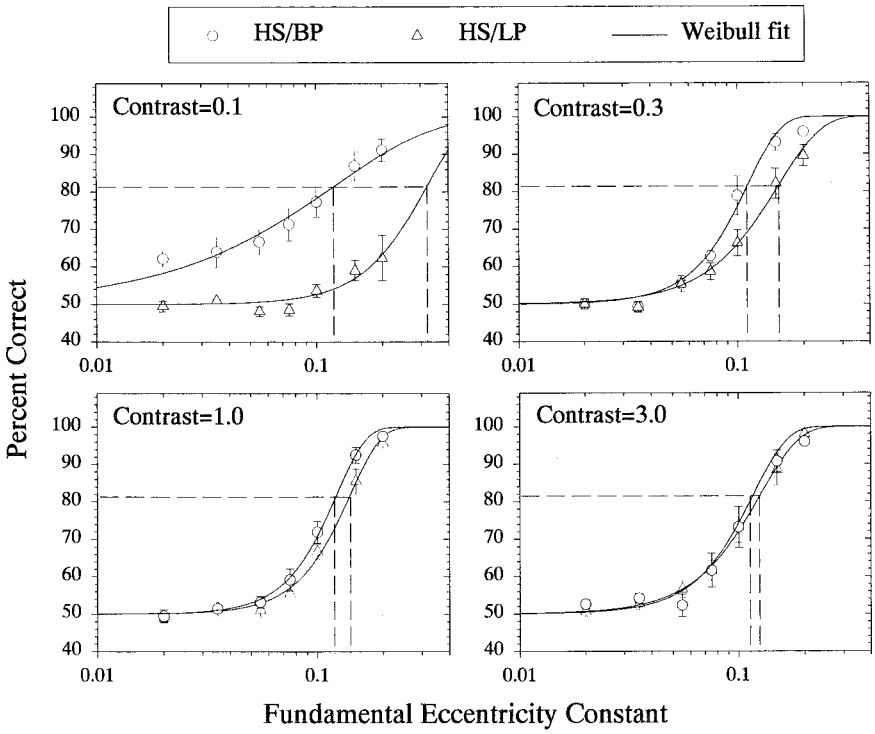

Fig. 6. Effect of image contrast on the threshold FEC level. Reducing the contrast of the test images increased the threshold FEC for the images processed with the high-sensitivity/low-pass (HS/LP) CSF but not with the high-sensitivity/bandpass (HS/BP) CSF. The error bars are ±1 s.e.m. intervals.

4. DISCUSSION

A. Effects of the High-Frequency Residual

Our initial attempt to compare test images produced with different CSF's[21,22] resulted in the unexpected finding of greater than chance (i.e., 50%) discrimination even at the lowest FEC levels (see Fig. 3, top graph). Such a result is possible since even for an FEC of zero, the images are processed with the foveal CSF [see Eq. (1)]. However, it should be noted that for the lower FEC levels, the images were processed so little that they were difficult to distinguish even when foveally examined side by side with unlimited viewing time. We initially suspected that the high level of discrimination in the periphery was related to the time course of the presentation (200 ms, square-wave window).[23] However, changing the time course to a 500 ms Gaussian temporal window did not significantly change the results.

Another aspect of our initial results was that the planes test image was easier to discriminate from its original than was a comparable version of the city test image (see Fig. 3, lower graph). The present visual model cannot account for this aspect of the data because it includes no image-dependent parameters. We have seen similar effects in testing central vision.[12] In that case, the effects were attributed to an artifact due to the so-called high-frequency residual (HFR), which was removed from the test images but which remained in the original image. The HFR is the set of spatial frequencies at the corners of the square spatial frequency support, which are excluded when only a circularly symmetrical filter is used.[24] Peli[12] found that removal of the HFR resulted in the elimination of the image dependency as well as an improved performance at various viewing distances. The data shown in Fig. 4 were obtained from HS/BP and LS/LP images from which the HFR had been removed. As noted above, the data from only one observer showed consistent differences for the two images used (airport versus planes). Further, the differences for this one observer tended to appear only for the more highly processed images (i.e., those with higher FEC values), suggesting that the difference was due to a criterion difference in judging the images rather than to differences in threshold discrimination. The same subject showed the same image dependence for the data collected with the test images generated by using the HS/LP CSF data.

B. Effects of the Model CSF on the Threshold FEC Level

1. Validity and Limitations of the Testing Method

Peli *et al.*[11] found that most peripheral CSF's reported in the literature could be represented with a foveal CSF and an FEC of ~0.05. Therefore in our earlier studies[21,22] as well as in the present study a range of FEC's was chosen to span the 0.05 level. Nevertheless, it would not have been surprising, with test stimuli obtained by using only the foveal CSF and one eccentricity parameter, to find that the test images associated with this range of FEC's were either all distinguishable or all indistinguishable from the original. The finding that by varying a single parameter of the model, the FEC, we can vary discrimination gradually from chance level to 100% confirms both the validity of the model and the fundamental role of the FEC in the discrimination of wide-field imagery. The fact that wide-field test images obtained with various foveal CSF's are discriminated at different FEC levels extends to peripheral vision our previous findings[12] regard-

ing the sensitivity of both the model and the testing method to small differences in the form of the model CSF.

The data of Fig. 5(b) show that, for all FEC levels, the test images obtained with the HS/LP CSF were more difficult to distinguish from the original image than were the test images obtained with the LS/LP CSF. This result is consistent with the relative sensitivity of the HS/LP and LS/LP CSF's over the spatial-frequency range typical of natural imagery [see Fig. 2(b)]. In applying the present model [see Eq. (1)], image points that were below threshold were processed (i.e., set to zero), whereas those above threshold were not. As a result, applying the higher-sensitivity (i.e., lower-threshold) HS/LP CSF resulted in more above-threshold image points and hence less overall processing and lower discrimination levels, as shown in the data of Fig. 5(b).

Although the data of Fig. 5(b) suggest that overall contrast sensitivity is a relevant factor in determining the discrimination of the wide-field images of the present study, the foveal CSF's used in the present study were complete functions of contrast sensitivity in that they differed in bandpass characteristics (i.e., shape) as well as in overall (maximal) sensitivity. For example, the HS/LP CSF is low pass, whereas the HS/BP CSF is bandpass, and in addition the two CSF's show similar sensitivity over only a restricted range of spatial frequencies while diverging at both higher and lower spatial frequencies. It might therefore be possible to determine more precisely the spatial frequency band underlying the present data by comparing the discrimination of images processed with these two CSF's. The data in Fig. 5(a) show that the test stimuli obtained with the HS/LP and HS/BP CSF's were equally difficult to distinguish from the original image. It appears, therefore, that in the context of the present visual model, the bandpass characteristic of the underlying CSF is relatively unimportant. Further, the HS/LP and HS/BP CSF's converge at spatial frequencies from approximately 2–4 c/deg, suggesting that this frequency range is responsible for mediating the differences in discrimination that are evident in Fig. 5(b). Thus the image spectrum designated with a contrast of one (C = 1.0) is illustrated in Fig. 2(c) to intersect the HS/LP and HS/BP CSF's where they intersect each other. Peli[13] has also noted that whereas the whole CSF is used to produce the test stimuli, only a very narrow range of frequencies (probably near the contrast sensitivity peak) is tested in the image discrimination task.

2. Varying Image Contrast to Test the CSF's at Various Spatial Frequencies

As discussed above, the discrimination data of Fig. 5(a) suggest that the portion of the image spectrum that was used in the present discrimination task coincides with the intersection of the HS/BP and HS/LP CSF's. However, there is nothing in the data of Fig. 5(a) that independently determines the location of the image amplitude spectrum relative to the CSF's, nor could this be determined by directly measuring the amplitude spectrum. As was noted above, the HS/LP and HS/BP CSF's differ at spatial frequencies below ~1 c/deg and above ~10 c/deg. The discrimination data shown in Fig. 6 for the original image (C = 1.0) show little difference between the HS/LP and HS/BP conditions. This result essentially replicates, with a different set of observers, the previously obtained data shown in Fig. 5(a). This finding is a further indication that the image amplitude spectrum intersects the HS/LP and HS/BP CSF's near the point where their sensitivities are equal.

There was also little change in discrimination performance when the contrast of the test images was increased (Fig. 6, C = 3.0). This can be explained by the fact that the difference between the HS/LP and the HS/BP CSF's is relatively small at the point where they intersect the C = 3.0 amplitude spectrum. Furthermore, both the spatial frequency content of the test images (see Section 2) and the sensitivity of the visual system at the eccentricities tested here (i.e., 6.4°–32°) are relatively low in the spatial frequency range at or above where the C = 3.0 amplitude spectrum intersects the HS/LP and HS/BP CSF's [see Fig. 2(c)].

Since the HS/LP CSF has a higher sensitivity than the HS/BP CSF at lower spatial frequencies, which are tested by low-contrast images, we might expect that a higher FEC would be required for the HS/LP images to match the original, unprocessed image. If this were the case, we would predict that the FEC's estimated from the HS/LP and HS/BP test stimuli would diverge if images of lower or higher contrast were used to test lower and higher frequencies, respectively. The data of Fig. 6 are consistent with this interpretation in that they show that when the contrast of the test images was progressively reduced (C = 0.3 and 0.1), the FEC estimated for the HS/BP condition remained largely unchanged,[25] whereas the FEC estimated for the HS/LP condition progressively increased. This finding suggests that peripheral sensitivity is better represented by the HS/BP function than by the HS/LP function, actually decreasing at lower spatial frequencies, and is also consistent with the placement of the amplitude spectra illustrated in Fig. 2(c), though we have no direct way to determine that placement.

5. CONCLUSIONS AND IMPLICATIONS

Taken together, the results summarized in Figs. 5 and 6 indicate that a single, eccentricity-dependent parameter (i.e., the FEC) is sufficient to model the spatial nonuniformity of the visual system as it relates to the discrimination of complex, wide-field images. Further, the HS/BP CSF was found to produce changes in the present test images, which resulted in FEC estimates that remained the same for large changes in image contrast. This suggests that the HS/BP CSF best characterizes the peripheral visual discrimination performance tested in the context of the present visual model.

The HS/BP CSF was found to give the best fit to the discrimination data of the present peripheral vision study, whereas the HS/LP CSF best described performance in the previous foveal study.[12] This apparent inconsistency can be explained by noting that there was little or no overlap among the retinal spatial frequencies that determined the results of the two studies. It is likely that only low frequencies were tested in the present study and that only high retinal frequencies were tested in the previous foveal study. Although we have not con-

firmed this directly, if it were indeed the case it would mean that the CSF that accounts for the performance in the discrimination task derives its low frequencies from the HS/BP CSF and its high frequencies from the HS/LP CSF.

All FEC's found here are larger than those computed from CSF's measured directly at various retinal eccentricities (see Table 1 in Ref. 11). This difference may be due to crowding or lateral masking effects produced by superimposed or adjacent image detail. Such effects may result in a more rapid decline of detection performance as retinal eccentricity is increased. Although such effects were demonstrated in a number of letter acuity tests, we are not aware of direct measurements of such lateral masking for gratings or grating patches. However, Lauritzen *et al.*[26] found that Gabor patches require higher contrast to be detected in image sections that contain high-contrast information.

The vision model employed here produced images that were discriminable in a way predictable from well-established visual and perceptual data. It might therefore be expected that analogous models could be employed to assess more general image properties such as perceived image quality. In particular, the peripheral-vision model suggested by the present analysis might be useful in evaluating wide-field simulator images as well as area-of-interest, or other, foveating systems. Our technique could be used, for example, to evaluate and calibrate the foveation software developed by Geisler and Perry.[27]

ACKNOWLEDGMENTS

This work was supported in part by grants EY05957, EY10285, and EY12890 from the National Institutes of Health, and by U.S. Air Force contract F41624-97-D-5000 to Raytheon Technical Services Company (now L3 Communications Corporation) at the U.S. Air Force Research Laboratory, Mesa, Arizona. We thank Brian Sperry, Jack Nye, and Craig Vrana for programming support.

Address correspondence to E. Peli at The Schepens Eye Research Institute, 20 Staniford Street, Boston, Massachusetts 02114, or by e-mail: eli@vision.eri.harvard.edu.

REFERENCES AND NOTES

1. A. P. Ginsburg, "Visual information processing based on spatial filters constrained by biological data," Ph.D. dissertation (Cambridge University, Cambridge, UK, 1978).
2. B. L. Lundh, G. Derefeldt, S. Nyberg, and G. Lennerstrand, "Picture simulation of contrast sensitivity in organic and functional amblyopia," Acta Ophthalmol. (KbH) **59**, 774–783 (1981).
3. D. Pelli, "What is low vision?" Videotape, Institute for Sensory Research, Syracuse University, Syracuse, N.Y. (1990).
4. L. N. Thibos and A. Bradley, "The limits of performance in central and peripheral vision," in Vol. 22 of Society for Information Display Digest of Technical Papers (Society for Information Display, Santa Ana, Calif., 1991), pp. 301–303.
5. J. Larimer, "Designing tomorrow's displays," NASA Tech. Briefs **17**(4), 14–16 (1993).
6. J. Lubin, "A visual discrimination model for imaging system design and evaluation," in *Vision Models for Target Detection*, E. Peli, ed. (World Scientific, Singapore, 1995), pp. 245–283.
7. E. Peli, R. B. Goldstein, G. M. Young, C. L. Trempe, and S. M. Buzney, "Image enhancement for the visually impaired: simulations and experimental results," Invest. Ophthalmol. Visual Sci. **32**, 2337–2350 (1991).
8. E. Peli, "Contrast in complex images," J. Opt. Soc. Am. A **7**, 2032–2040 (1990).
9. S. Daly, "The visual differences predictor: an algorithm for the assessment of image fidelity," in *Human Vision, Visual Processing, and Digital Display III*, B. E. Rogowitz, ed., Proc. SPIE **1666**, 2–15 (1992).
10. M. Duval-Destin, "A spatio-temporal complete description of contrast," in Vol. 22 of Society for Information Display Digest of Technical Papers (Society for Information Display, Santa Ana, Calif., 1991), pp. 615–618.
11. E. Peli, J. Yang, and R. Goldstein, "Image invariance with changes in size: the role of peripheral contrast thresholds," J. Opt. Soc. Am. A **8**, 1762–1774 (1991).
12. E. Peli, "Test of a model of foveal vision by using simulations," J. Opt. Soc. Am. A **13**, 1131–1138 (1996).
13. E. Peli, "Contrast sensitivity function and image discrimination," J. Opt. Soc. Am. A **18**, 283–293 (2001).
14. E. L. Schwartz, "Spatial mapping in the primate sensory projection: analytic structure and relevance to perception," Biol. Cybern. **25**, 181–194 (1977).
15. A. B. Watson, "Estimation of local spatial scale," J. Opt. Soc. Am. A **4**, 1579–1582 (1987).
16. A. Johnston, "Spatial scaling of central and peripheral contrast-sensitivity functions," J. Opt. Soc. Am. A **4**, 1583–1593 (1987).
17. J. S. Pointer and R. F. Hess, "The contrast sensitivity gradient across the human visual field with emphasis on the low spatial frequency range," Vision Res. **29**, 1133–1151 (1989).
18. M. W. Cannon, Jr., "Perceived contrast in the fovea and periphery," J. Opt. Soc. Am. A **2**, 1760–1768 (1985).
19. W. Weibull, "A statistical distribution function of wide applicability," J. Appl. Mech. **18**, 293–297 (1951).
20. The curve fitting was done with the SigmaPlot Scientific Graph System (Jandel Scientific).
21. E. Peli and G. Geri, "Putting simulations of peripheral vision to the test," Invest. Ophthalmol. Visual Sci. **34** (ARVO Suppl.), 820 (1993).
22. E. Peli, "Simulating normal and low vision," in *Vision Models for Target Detection and Recognition*, E. Peli, ed. (World Scientific, Singapore, 1995), pp. 63–87.
23. E. Peli, L. Arend, G. Young, and R. Goldstein, "Contrast sensitivity to patch stimuli: effects of spatial bandwidth and temporal presentation," Spatial Vis. **7**, 1–14 (1993).
24. A. B. Watson, "The cortex transform: rapid computation of simulated neural images," Comput. Vision Graph. Image Process. **39**, 311–327 (1987).
25. Under the HS/BP condition, the psychometric function for $C = 0.1$ was found to have a shape different from those obtained at the other contrast levels. The slope of the psychometric function may be related to the underlying signal to noise level, and thus it is not surprising that reducing the image contrast resulted in a flatter function with little or no change in the threshold FEC value.
26. J. S. Lauritzen, S. M. Hood, D. J. Tolhurst, Y. Tadmor, and A. Pelah, "Detection of Gabor patches embedded in natural images," Perception **27**, 151–152 (1998).
27. W. S. Geisler and J. S. Perry, "A real-time foveated multiresolution system for low-bandwidth video communication," in *Human Vision and Electronic Imaging III*, B. Rogowitz and T. Pappas, eds., Proc. SPIE **3299**, 294–305 (1998).